3D-QSAR Studies of Arylpyrazole Antagonists of Cannabinoid Receptor Subtypes CB1 and CB2. A Combined NMR and CoMFA Approach

Jian-Zhong Chen,[†,‡] Xiu-Wen Han,[‡,§] Qian Liu,[‡] Alexandros Makriyannis,[‡,||,⊥] Junmei Wang,[†] and Xiang-Qun Xie*,[†,‡]

Department of Pharmaceutical & Pharmacological Sciences, College of Pharmacy, University of Houston, 4800 Calhoun Rd., Houston, Texas 77204-5037, and Department of Pharmaceutical Sciences and Molecular & Cell Biology, Center for Drug Discovery, School of Pharmacy, University of Connecticut, 69 N Eagleville Rd., Storrs, CT 06269-3092

The present work focuses on the study of the three-dimensional (3D) structural requirements for selective antagonist activity of arylpyrazole compounds at the cannabinoid CB1 and CB2 receptors. Initially, a combined high-resolution two-dimensional (2D) NMR and computer modeling approach was carried out to study the solution structure of the key pyrazole derivative *N*-(piperidin-1-yl)-5-phenyl-1-(*n*-pentyl)-4-methyl-1*H*-pyrazole-3-carboxamide (AM263). By using the NMR-determined molecular conformers as templates, the 3D quantitative structure−activity relationship (QSAR) studies were performed with the comparative molecular field analysis (CoMFA) approach on a set of arylpyrazole cannabinoid receptor antagonists. Molecular alignments suitable for deriving valuable pharmacophoric features for this series of compounds were determined. Such systematic 3D-QSAR/CoMFA analyses of 29 molecules and their receptor affinities gave guidance for understanding the binding affinities of arylpyrazoles at the CB1 and CB2 binding sites, respectively. Comparison of CoMFA steric and potential contour maps for affinity at the two cannabinoid receptor subtypes helps to differentiate structural requirements for each subtype and serves as a basis for the design of later-generation analogues.

Introduction

The CB1 cannabinoid receptor (CB1) is expressed in the central nervous system (CNS) and other tissues,[1−3] while the peripheral CB2 cannabinoid receptor (CB2) is expressed in the immune system[4,5] and is involved in cannabinoid-mediated immune responses. The two receptors were identified as a subgroup of the G-protein coupled seven-transmembrane-spanning receptor family.[2] Since their discovery, cannabinoid research has witnessed rapid and important developments. Pharmacological studies have shown that cannabinoids possess many potential therapeutic applications, including cancer chemotherapy, AIDS, pain relief, muscle spasms, glaucoma, immune suppression, etc.[6−11] Furthermore, efforts have been devoted toward designing novel CB1 ligands possessing potent analgesic properties but devoid of the psychotropic effects of marijuana, as well as CB2 ligands possessing immunomodulatory properties but devoid of CNS effects.[12−14] However, many unanswered questions regarding the molecular interactions between the receptors and their ligands as well as the nature of each receptor's active site(s) remain to be addressed.

Thus far, more than five structurally diverse sets of cannabinergic ligands have been discovered,[13] including classical cannabinoids, nonclassical cannabinoids, aminoalkylindoles, eicosanoids, and arylpyrazoles (Figure 1). Most known cannabinoids, including the naturally occurring (e.g., Δ[9]-THC, anandamide) and synthetic cannabinoid ligands (e.g., CP-55940, WIN55212-2), do not exhibit substantial selectivity for the CB1 or CB2 receptors. Efforts to develop cannabinoid-based medica-tions have involved extensive chemical modifications of cannabinoid structures in order to dissect the medicinal properties of these compounds away from their undesirable psychotropic effects. The discovery of additional cannabimimetic compounds, whose structures differ from the classical and nonclassical cannabinoids, have enhanced this effort and led to greater diversity in cannabinergic lead structures.

Reported here are the results of studies on three-dimensional (3D) quantitative structure−activity relationship (QSAR) models of arylpyrazoles using the comparative molecular field analysis (CoMFA)[15] approach in combination with two-dimensional (2D) NMR spectroscopy. CoMFA has been widely used to extract indirect information on receptor site structure by aligning structurally similar analogues using pharmacophoric features as structural superimposition guides.[14] In this method, the steric and electrostatic fields are computed on the basis of the 3D molecular conformation of each ligand in the training set. The 3D-QSAR models are then constructed by correlating the steric and electrostatic fields with the corresponding observed binding affinities of ligands for each receptor subtype.

CoMFA studies have been carried out to develop the 3D-QSAR models of the different classes of cannabinoid ligands for their cannabinoid receptor binding profiles. These efforts include classical and nonclassical cannabinoids,[16,17] aminoalkyl-indoles,[18] eicosanoids,[19,20] and arylpyrazoles.[21] Most of these 3D-QSAR studies were focused on the CB1 receptor,[16−21] whereas only one study has reported CoMFA models for both CB1 and CB2 receptors.[22] This study used the same training set of 20 compounds with representatives from all five classes of cannabinergic ligands. However, a variety of biochemical and pharmacological data suggest that the different classes of cannabinoid ligands may interact with cannabinoid receptors that have different binding motifs. For example, a K3.28(192)A mutation study of the CB1 receptor revealed that the residue K3.28(192) is crucial for the binding and activation produced by classical or nonclassical cannabinoids but not for aminoalkyl-

* To whom correspondence should be addressed: Tel: 713-743-1288. Fax: 713-743-1229. E-mail: xxie@uh.edu.

† Department of Pharmaceutical & Pharmacological Sciences, University of Houston.

‡ Department of Pharmaceutical Sciences, University of Connecticut.

§ Current address: Dalian Institute Chemical Physics, 457 Zhongshan Rd., Dalian, Liaoning 116023, P. R. China.

|| Molecular & Cell Biology, University of Connecticut.

⊥ Center for Drug Discovery, University of Connecticut.

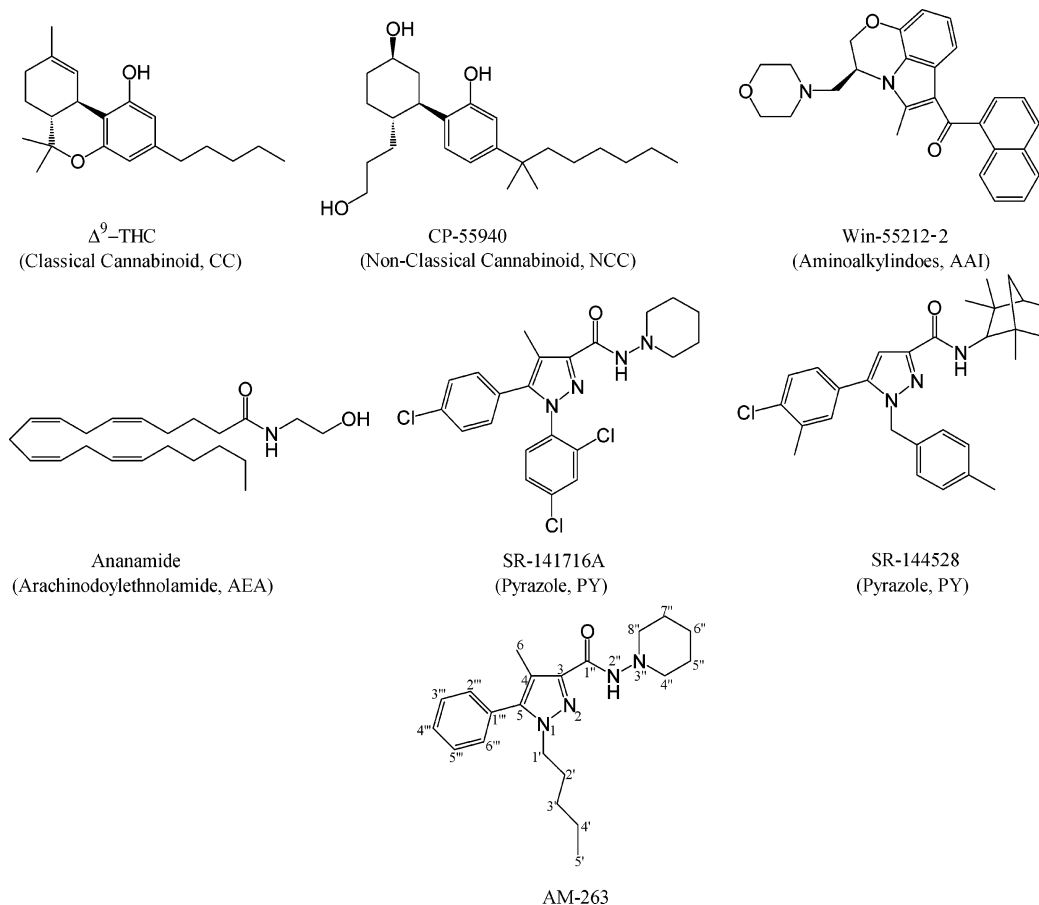**Figure 1.** Molecular structures of representative cannabinoid agonists and antagonists.

indoles.[23] In addition, the comparative receptor binding analyses of cannabinoid agonists and antagonists suggest that the cannabinoid agonists interact with binding sites of the receptor, which are distinguishable from binding sites of cannabinoid antagonists.[24] Therefore, attempts to construct active pharmacophore models by structural superposition of compounds encompassed in the structurally dissimilar cannabinergic classes can lead to ambiguous interpretations.[14]

Arylpyrazoles, represented by SR141716A and SR144528 (Figure 1), were the first selective pyrazole CB1 and CB2 receptor antagonists developed by Sanofi.[25,26] Since their discovery, extensive studies have been performed on the chemical modification of the arylpyrazoles.[27−32] These structure−activity relationship (SAR) studies were used to develop quantitative[21] or qualitative[24,33] SAR models for the arylpyrazoles binding to the CB1 receptor.

In the present study, we have carried out CoMFA studies combined with 2D NMR results in order to establish CB1 and CB2 3D-QSAR models and to correlate the structural differences of arylpyrazole analogues with the respective variations observed in their CB1 or CB2 binding affinities. The project first involved the use of 2D high-resolution NMR and computer modeling techniques to study the conformational properties of *N*-(piperidin-1-yl)-5-phenyl-1-(*n*-pentyl)-4-methyl-1*H*-pyrazole-3-carboxamide (AM263) (Figure 1), a high-affinity arylpyrazole analogue developed in the Makriyannis laboratory. The preferred solution conformation of AM263 was determined by the maximum agreement of NOESY NMR data and a computer-assisted conformational search. On the basis of the binding affinities of compounds of a training set,[28,33] CoMFA analysis was performed to build the 3D-QSAR models for the arylpyrazole binding motifs with the CB1 and CB2 receptors, respec-

tively, by structurally aligning all of the compounds in the training set onto the NMR-determined templates. Subsequently, each generated 3D-QSAR model allowed us to predict the K_i values (calculated K_i) of the arylpyrazoles. Statistical analyses of the data were used to determine linear correlation coefficients between calculated versus actual affinities. Comparisons of the CoMFA contour plots could then be used to elucidate different structural requirements for the CB1 and CB2 receptors based on the arylpyrazole binding. The CoMFA contoured trends can then be used as guides for designing novel, more selective, and higher affinity analogues. In addition, the 3D-QSAR models provide a means for predicting the affinities of untested compounds.

Materials and Methods

Materials. The synthesis of AM263 will be described elsewhere. Deuterated chloroform (CDCl$_3$) and tetramethylsilane (TMS) were purchased from Aldrich Chemical Co. (Milwaukee, WI). NMR samples were prepared as 0.02 M solutions in CDCl$_3$, thoroughly degassed with the freeze−thaw method, and sealed in high-quality 5-mm NMR tubes. TMS was used as an internal chemical shift reference.

NMR Spectra. High-resolution ^{1}H NMR spectra were collected on a Bruker AVANCE DMX500 spectrometer with a 5-mm inverse detection triple resonance probe and a BVT-2000 temperature controller. Two-dimensional phase-sensitive ^{1}H−^{1}H COSY spectra (COSYPHDQF)[34] were recorded with the following acquisition parameters: 90° pulse width, 6.2 μs; spectral width, 3623.19 Hz; recycling delay (D1), 2 s; temperature, 298 K. The data sizes were 512w in f1 and 2K in f2 and were zero-filled in f1 prior to 2D Fourier transformation to yield a 2K × 2K data matrix. The spectra were processed using a qsine-bell function in f1 and f2. In 2D ^{1}H−^{1}H phase-sensitive NOESY (NOESYPH)[35] experiment was per-

formed using acquisition parameters similar to the COSYPHDQF, with the addition of mixing times of 400 and 800 ms. 2D ^{1}H$-^{13}$C inverse correlated experiments with heteronuclear multiple quantum coherence (HMQC)[36] were performed using the inverse detection probe with the following acquisition parameters: 90° and 180° pulses, 6.2 and 12.4 μs for ^{1}H and 14.5 and 29.0 μs for ^{13}C; decoupling low power, 11 dB; J_{C-H} value delay time, 3.57 ms; delay for bilinear rotation decoupling (BIRD) inversion pulse, 0.35 s; increment, 9 μs; for ^{1}H, SI2 = 1024k, TD2 = 512w, SW = 3623.19 Hz; for ^{13}C, SI1 = 4096k, TD1 = 1024k, SW = 178 ppm. Two-dimensional ^{1}H$-^{13}$C inverse correlated experiments with heteronuclear multiple bond correlation (HMBC)[37] were conducted using similar acquisition parameters as HMQC while choosing a proper delay time (50 ms) to enhance the observation of selected long-range coupling (e.g. $^2J_{C-H}$, $^3J_{C-H}$, and $^4J_{C-H}$).

Computer Molecular Modeling. Molecular modeling was carried out with the Tripos Sybyl molecular modeling package[38] on an SGI Octane R10000 workstation. Molecular dynamic (MD) and mechanic (MM) simulations were utilized to examine the motions of molecular fragments and then to sample various molecular conformations at the local minima of the energy landscape. The starting structure of AM263 was first built by using the standard bond lengths and angles from the Sybyl molecular modeling package and was further minimized with the Tripos force field. Molecular dynamic simulations were performed at 1000 K using the Tripos force field with the time steps being set to 1 fs. It is known that the Tripos force field has the missing force field parameters between the acyl hydrazide nitrogen and nonacylated hydrazide nitrogen. We have modified the force field by implementing the new parameters from X-ray crystal structures of *N,N*-dimethyl-*N'*-(*o*-fluorobenzoyl)hydrazide[39] and *N',N'*-dibenzylbenzohydrazide.[40] The protocol for molecular conformation simulation is briefly described as follows: (1) The initial structure was first relaxed by performing a 100-step minimization with the maximum derivative being set to 0.1 kcal·mol^{-1}·Å^{-1}. (2) Molecular dynamics simulation at a high temperature of 1000 K was then carried out to efficiently cross the energy barriers and sample local minima. Three hundred snapshots were collected at a rate of 1 ps/snapshot for postprocessing analysis. (3) The 300 collected snapshots were further minimized with the steepest descent and followed by the conjugate gradient methods until the maximum derivative was less than 0.001 kcal·mol^{-1}·Å^{-1}.

Structural Alignment. In the present study, the same training set containing 29 arylpyrazole compounds (Table 1), most of which were developed to serve as cannabinoid antagonists in the Makriyannis laboratory,[28,33] was used for parallel CoMFA analyses to build 3D-QSAR models based on the experimentally determined binding affinities of the arylpyrazole analogues for the CB1 and CB2 receptors. Two additional arylpyrazoles, SR141716A and SR144528, were also included in the training set to enhance the structural alignment. This strategy allows for a direct comparison of 3D-QSAR models for the CB1 and CB2 receptors. For the CoMFA analysis of arylpyrazoles binding to the CB1 receptor, structural alignment of all compounds in the training set was performed using the various conformations of AM263 as templates. Only 28 compounds (excluding the CB2 K_i value for compound **4**) had experimentally determined affinities for CB2 and thus were chosen for alignment in order to construct the 3D-QSAR model of ligand binding affinity for the CB2 receptor. Another nine compounds were chosen from published articles and patents [28,32,41] to compose the test set (Table 2) for the evaluation of the constructed 3D-QSAR models.

Structures of other compounds in the training set were constructed by modifying the AM263 structure using the molecular fragments library provided within Sybyl.[38] The constructed conformers of each compound were then energy-minimized using the Tripos force field with a distance-dependent dielectric function and a convergence criterion of 0.001 kcal·mol^{-1}·Å^{-1} energy difference between successive iterations. The partial atomic charges, which were used to calculate the electrostatic interactions, were assigned on the basis of the Gasteiger–Hückel formalism.
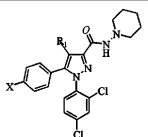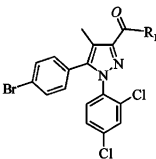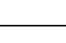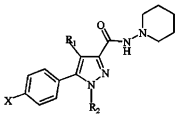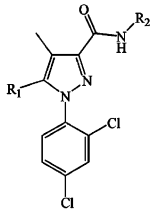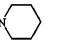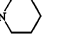
Because of their close structural similarity, we have assumed that all of the compounds under study interact with each of the two receptors through the same binding motifs; structural alignment is required both for both pharmacophore map determination and as a necessary step in CoMFA analysis. The model can then test hypotheses regarding the specific "bound" conformational alignment from all chosen conformations. AM263 was selected as the template for molecular superimposition because it exhibits high affinities for both CB1 and CB2 receptors. A conformational study of AM263 was then carried out using 2D NMR. on the basis of the reported SAR analyses of the arylpyrazole compounds,[33] four pharmacophoric groups were selected as a basis for the structural alignment of all ligands: the pyrazole ring; the C, N, and O atoms of the *N*-piperidin-1-yl amide group; the phenyl ring; and the non-hydrogen atoms of the pentyl group. It is reasonable to assume that ligands do not necessarily bind to the receptors in their global minimum energy conformations because some degree of bond rotation may be required to adapt electrostatic and hydrogen-bonding distances that would yield the lowest energy drug–receptor complex. Thus, the "minimum" energy conformations obtained from the previous MAXIMIN2 procedure are only useful starting points for finding the possible binding conformation candidates of the compound. On the other hand, it is important to note that the allowed pharmacophoric conformations of the different compounds must be restricted to those that can be obtained upon binding within reasonable energy limits. Typically, a 10 kcal·mol^{-1} cutoff difference between the local minimum and the aligned conformational energy of each compound was acceptable for superimposition in structural alignment.
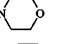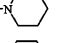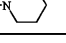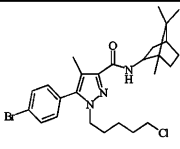
CoMFA Partial Least-Squares (PLS) Analysis. The CoMFA study was carried out by running the SYBYL/CoMFA module. The steric and electrostatic field energies (AM1 charge) were calculated using a sp^3 carbon probe atom with a charge of +1 and a distance-dependent dielectric constant in all intersections of a regularly spaced (0.2 nm) grid. Steric and electrostatic contributions were truncated at 30 kcal·mol^{-1}. All initial partial least-squares (PLS) analyses were performed using the "leave-one-out" cross-validation method. A minimum σ (column filter) value of 2.00 kcal·mol^{-1} was set to improve the signal-to-noise ratio by omitting those lattice points whose energy variation was below this threshold. The final model (non-cross-validated conventional analysis) was developed from the model with the highest cross-validated r^2, and the optimum number of components was set to equal that yielding the highest r_{cv}^2.

Results

NMR Spectral Assignments. The ^{1}H and ^{13}C spectral assignments of AM263 were made on the basis of the *J* coupling connectivities in the ^{1}H$-^1$H DQF-COSY spectrum and ^{1}H$-^{13}$C HMQC spectrum. The chemical shifts for the *n*-pentyl group and phenyl ring protons were determined on the basis of proton integration and analysis of the expanded regional contour plots of the phase sensitive DQF-COSY and HMQC spectra. A logical starting point is from the H5′ proton of the *n*-pentyl group. This can be readily identified in the ^{1}H spectrum, as a triplet at 0.80 ppm with an integration of three protons. Having assigned the H5′, the H4′ (1.18 ppm), H3′ (1.11 ppm), H2′ (1.68 ppm), and H1′ (3.93 ppm) were then identified on the basis of connectivity in the DQF-COSY spectrum. Following the H1′ assignment, C5 was assigned at 142.67 ppm by identifying the $^3J_{H1'-C5}$ coupling, H6 at 2.21 ppm by $^3J_{H6-C5}$, and protons 2‴,6‴ at 7.24 ppm by $^3J_{H2'''-6'''-C5}$ in the 2D ^{1}H$-^{13}$C HMBC spectrum. Subsequently, H3‴,5‴ and H4‴ were identified on the basis of their connectivities with the 2‴, 6‴ protons in the 2D DQF-COSY spectrum. Assignment for the piperidine ring protons is more straight forward and is based on their chemical environments and peak integration. Chemical shifts were further confirmed by comparing the DQF-COSY, HMQC, and HMBC

Table 1. Molecular Structures and Binding Affinity K_i Values of Arylpyrazoles Analogues Used as the Training Set to Construct CoMFA Models[28,33]

No.	X	R_1	R_2	K_i (nM) CB1	K_i (nM) CB2
1(SR141716A)	Cl	CH_3	-	11.5	1643.0
2	Cl	H	-	37.9	731.0
3	H	CH_3	-	122.7	216.5
4	H	H	-	202.0	-
5	-	[pyrrolidine]	-	17.1	1301
6	-	[piperidine]	-	16.8	1426
7	-	[azepane]	-	7.18	719
8	-	[CH3 piperidine]	-	76.7	1259
9	-	[piperidine]	-	124.9	4568
10	-	[NMe piperazine]	-	168.1	1.1e+4
11	-	[phenyl hydrazide]	-	158	3.1e+4
12	Cl	CH_3	CH_3	3.5e+4	5.32e+4
13	H	CH_3	n-C_3H_7	3563	1541
14(AM263)	H	CH_3	n-C_5H_{11}	11.14	26.83
15	H	CH_3	n-C_7H_{15}	204.1	342.3
16	H	CH_3	Cyclohexyl	605.8	1444
17	Br	CH_3	n-C_5H_{11}	81.8	526.7
18	H	H	n-C_5H_{11}	256.6	90.27
19	H	H	n-C_7H_{15}	327.3	84.1
20	Cl	CH_3	o-ClC_6H_5	59.7	835.5
21	-	C_2H_5	[piperidine]	183	744.2
22	-	o-$NO_2C_6H_5$	[piperidine]	57.5	252.4
23	-	o-$NH_2C_6H_5$	[piperidine]	81.5	958
24	-	o-IC_6H_5	[morpholine]	13.24	4207
25	-	o-BrC_6H_5	[piperidine]	11.67	1011
26	-	o-IC_6H_5	[azepane]	7.49	2293
SR144528 27	-	-	-	400	0.6
28	-	-	-	5.01	75.7
29	-	-	-	5.98	2.51

spectra. The same chemical shifts were observed between the cyclohexyl protons H4″ and H8″ as well as H5″ and H7″, and in addition the undistinguishable axial and equatorial protons of these piperidine ring CH_2 groups were located at 2.90 and 1.74 ppm, respectively. All these indicated that piperidine ring underwent ring conversion. Therefore, the conformations measured in this experiment will be time-averaged on the NMR time scale. Table 3 summarizes the complete assignments of proton and carbon chemical shifts for AM263.

NOE−Dipolar Interactions. Figure 2 shows the 2D ^{1}H−^{1}H phase-sensitive NOESY spectrum for AM263. The nuclear Overhauser effect (NOE) value is one of the most important NMR parameters used in conformational analysis, since the magnitude of the NOE is inversely proportional to the sixth power of the interproton distance in space ($I_{NOE} \propto r^{-6}$). Typically, an observed NOE cross-peak indicates that two protons are near in space within a 3.0 Å distance and exhibit through-space coupling. Beyond the 3.0 Å range, the NOE is

Table 2. Molecular Structures and Binding Affinity K_i Values of Compounds Were Used as the Test Set to Examine the CoMFA Models[28,32,41]
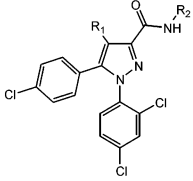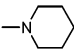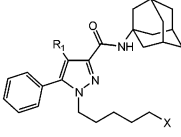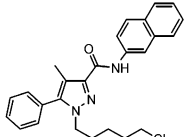

No.	X	R_1	R_2	K_i (nM) CB1	K_i (nM) CB2
T1	-	-CH$_3$	-CH$_2$CH$_3$	46.3±1.5	3110±610
T2	-	-CH$_3$	-(CH$_2$)$_3$OH	160±19	1250±280
T3	-	-CH$_3$	-NH$_2$	374±27	12100±170
T4	-	-CH$_3$	-NHC$_2$H$_5$	143±9	6061±900
T5	-	-CH$_2$CH$_3$	(piperidine)	3.5	442
T6	-Cl	-CH$_3$	-	1.42	0.784
T7	-Cl	-H	-	12.2	4.79
T8	-F	-CH$_3$	-	1.25	0.682
T9	-	-	-	14.6	15.4

Table 3. 500-MHz ^{1}H NMR and 125-MHz ^{13}C NMR Chemical Shift Assignments for AM263

hydrogen and carbon	δ (ppm) ^{1}H	δ (ppm) ^{13}C	hydrogen and carbon	δ (ppm) ^{1}H	δ (ppm) ^{13}C
3		142.67	1″		160.65
4		117.41	4″,8″	2.90	57.08
5		141.43	5″,7″	1.74	25.38
6	2.21	9.14	6″	1.43	23.30
1′	3.93	49.79	1‴		129.66
2′	1.68	29.92	2‴,6‴	7.24	129.85
3′	1.11	28.47	3‴,5‴	7.47	128.71
4′	1.18	22.08	4‴	7.45	128.71
5′	0.80	13.85	N−H	7.67	

very weak, and the effect becomes barely detectable at 5 Å.[35] Our data showed a strong NOE cross-peak between the amide proton (7.67 ppm) and the piperidine H4″,8″ (2.90 ppm) protons; the phenyl H2‴,6‴ (7.24 ppm) proton and methyl proton H6; the phenyl H2‴,6‴ proton and pentyl H1′ (3.93 ppm), H2′ (1.68 ppm), H3′ (1.11 ppm) protons; the pentyl H1′ (3.93 ppm) and H3′ (1.11 ppm); the pentyl H3′ (1.11 ppm) and H5′ (0.81 ppm); the pentyl H1′ (3.93 ppm) and H4′ (1.18 ppm); and the pentyl H2′ (1.68 ppm) and H4′ (1.18 ppm) as shown in Figure 2. The above NOE cross-peaks provide important information regarding the preferred orientation of the phenyl and piperidine rings with respect to the pyrazole ring.

Computer Modeling. Molecular dynamic/mechanic simulations were carried out to search for the preferred low-energy conformations of AM263. Dynamic motions were simulated at a high temperature (1000 K) to increase the probability of inducing conformational transitions past any possible high-energy barrier. The dynamic simulations were performed with time steps of 1 fs for 300 ps, and the data were recorded at 1-ps intervals with a total of 300 frames of conformers sampled. Molecular mechanics energy minimization was carried out for each of the 300 conformations. This operation resulted in a convergence of these conformers into six families represented in Figure 3 by six minimum-energy conformations which were

sampled during the dynamics simulation and then followed by energy minimization. The energy difference of these six conformers was less than 8 kcal·mol^{-1}. Table 4 summarizes the important interproton distances from the calculated conformations.

Preferred Conformation of AM263. Our study of the conformational properties of AM263 was performed by combining the NMR experimental results with computational data obtained from computer molecular mechanic/dynamic calculations. The preferred AM263 conformation with a proper alignment of pharmacophoric groups was determined by maximal agreement between the experimental and computational results. By analyzing the conformational properties of individual molecular components and subsequently combining them to provide a complete picture of the molecule, we were able to construct a conformational base for the CoMFA analysis.

In the ^{1}H−^{1}H NMR NOESYPH spectrum of AM263 (Figure 2), a strong NOE cross-peak was observed between the amide proton and H4″,8″ (2.90 ppm) of the piperidin-1-yl group. However, no NOE cross-peak was observed between the amide proton and the methyl of 4-methyl-1H-pyrazole, amide, and piperidine-1-yl H5″,7″ protons. The positive broad cross-peak at (7.67, 1.64 ppm) was attributed to the NIH chemical shift exchange with the impurity from commercial CDCl$_3$, but not a NOE cross-peak, which was described in the literature. [42] The observed NOEs provided evidence for the through-space relative distances of the above protons, a result that was used to deduce the relative orientation of the pyrazole and piperidine rings with respect to the amide group. As shown in Figure 3 and Table 4, the molecular modeling results showed that the interproton distances between the amide and C-6 methyl protons of 4-methyl-1H-pyrazole in conformers F36 and F115 and the distance between the amide proton and protons 5″,7″ of the piperidine ring protons in conformer F53 were lower than 2.5 Å. Since these distances are not congruent with the NMR data, we conclude that these two conformers are not represented to any significant extent in the NMR experimental data. For the
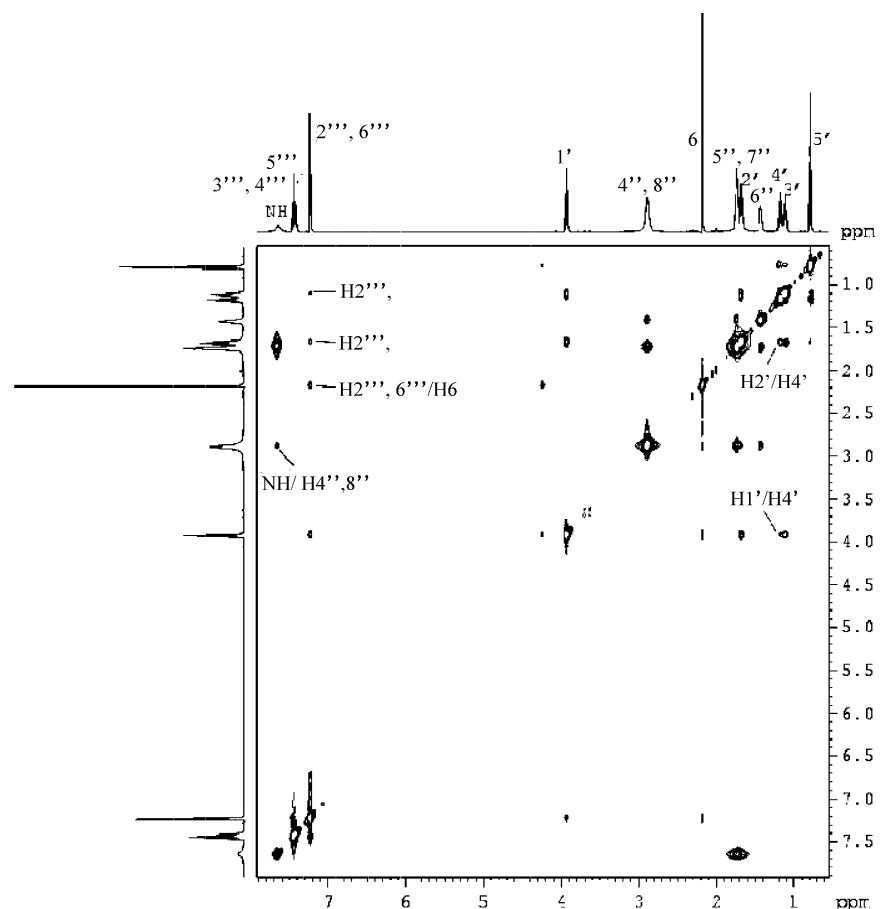
Figure 2. ¹H−¹H 2D NOESYPH NMR spectra (500 MHz) of AM263 in CDCl₃ solution at 298 K. The NOE interactions for AM263 indicated with arrows.
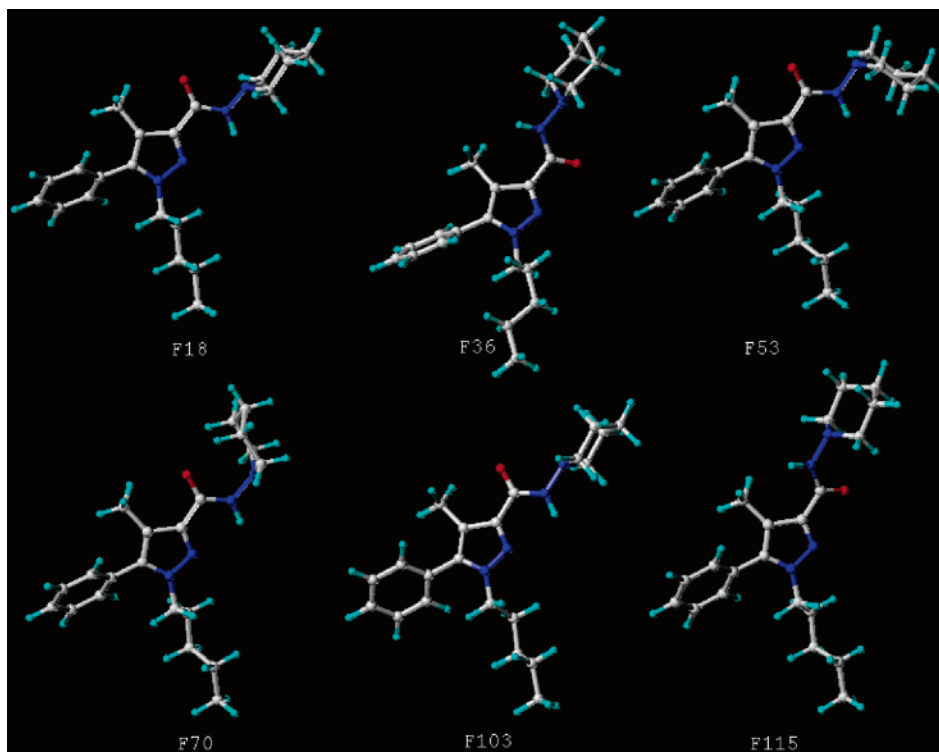
Figure 3. Molecular graphic representation of five favored conformations of AM263 on the basis of the energy minimization of structures occurring along the molecular dynamics trajectory.

F18 conformer, the interproton distance between H1′ and H4′ of the *n*-pentyl group is greater than 4.0 Å, whereas the ¹H−¹H NMR NOESYPH spectrum showed that a relatively strong NOE cross-peak was observed between these protons. Therefore, conformer F18 can also be ruled out as a major conformation in solution. The remaining conformers are F103 and F70, both

Table 4. Relative Energy (kcal/mol) and Interproton Distance[a] (Å) of Five Favored Conformations of AM263 on the Basis of the Energy Minimization of Structures Occurring along the Molecular Dynamics Trajectory

	E	1′−3′	3′−5′	1′−4′	2′−4′	2‴,6‴−1′	2‴,6‴−2′	2‴,6‴−3′	2‴,6‴−4′	2″,6‴-6	NH−6	NH−4″,8″	NH−5″,7″
F18	21.63	2.59	2.53	4.07	2.27	2.16	3.04	3.73	5.73	2.66	5.01	2.60	4.60
F36	25.61	2.68	2.52	2.61	2.56	2.90	2.51	4.79	3.46	2.55	2.50	2.60	4.58
F53	22.41	2.58	2.55	2.41	2.60	2.61	2.50	3.45	5.14	2.72	4.98	2.83	2.45
F70	25.40	2.56	2.55	2.42	2.60	2.62	2.49	3.39	5.10	2.72	4.97	2.89	4.22
F103	21.75	2.58	2.55	2.41	2.60	2.61	2.50	3.45	5.14	2.72	4.99	2.60	4.60
F115	25.17	2.58	2.54	2.41	2.59	2.61	2.49	3.45	5.14	2.64	2.48	3.06	4.43

[a] The calculated distances are usually referral to the shortest distance for the equivalent protons.

of which are congruent with the experimental data, with calculated H1′−H4′ distances of ∼2.4 Å. However, the molecular energy of conformer F70 is 3.5 kcal·mol^{-1} higher than that of conformer F103, due to a diaxial interaction between the amide NH and piperidine nitrogen lone pair electrons in F70. This led us to assume that conformer F103 is a preferred and representative conformation in chloroform as it has a maximum agreement with the NMR experimental data in solution.

CoMFA Analyses of Arylpyrazoles Binding to CB1 and CB2 Receptors. The CoMFA method was employed to build 3D-QSAR models for arylpyrazoles based on observed binding affinities (K_i values) for the CB1 and CB2 receptors. Since conformers F18 and F103 are very similar, except for the *n*-pentyl group showing an all-trans-conformation in F18 and a guache-conformer in F103, the conformers F36, F53, F70, F103, and F115 were separately selected as templates for alignment to carry out CoMFA analyses for the CB1 and CB2 receptors. On the basis of each template, we considered several variations in the alignment schemes by superimposing the four common or similar pharmacophoric features, which were detailed in the Materials and Methods. The best results involved not only a reasonably good overlap of the putative biologically relevant pharmacophore groups but also statistically significant 3D-QSAR models from CoMFA. For example, Figure 4 illustrates the structural superimpositions of 29 compounds for the CB1 and 28 for CB2 CoMFA analyses, respectively. To properly superimpose CB1 or CB2 ligands onto the selected template AM263, the N1-pentyl chain of AM263 was further explored in various gauche-conformations for the CB1 or CB2 CoMFA analyses, as an alkyl chain always has the highest flexibility in interaction with the receptor binding sites.

In all instances, cross-validated PLS analyses[43] were run to determine the optimal number of components in the model and to evaluate the robustness of the model based on how well it predicts data. A "cross-validated r_{cv}^2" or "predictive r_{cv}^2" can be defined as

$$\text{cross-validated } r_{cv}^2 = (SD - PRESS)/SD$$

where SD is the sum of the squared deviations of each biological property value from their mean, and PRESS is the sum, over all compounds, of the squared differences between the actual and "predicted" biological property values. The PLS analyses were repeated until the biological property value has been "predicted" by a model from where these were derived. There is a generally accepted criterion for CoMFA statistical validity of $r_{cv}^2 \geq 0.6$. Among all of our CoMFA analyses, only the CoMFA models for both CB1 and CB2 based on conformer F103 exceeded this criterion. Most of the other models failed to meet this criterion. Although the CoMFA models for CB1 based on the conformer F115 or for CB2 based on the conformer F36 also exceeded the criterion, their r_{cv}^2 values are still lower than the ones derived from the conformer F103. Furthermore,
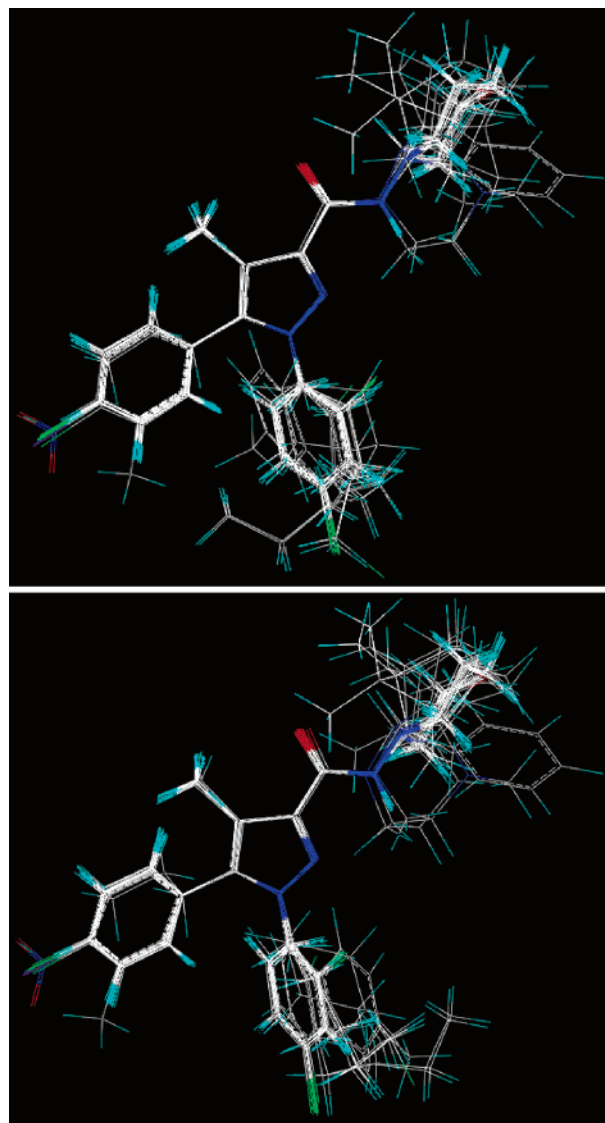
Figure 4. F103-based structural alignments of the compounds in the training set for building 3D-QSAR models of CB1 (top) and CB2 (bottom) by CoMFA.

the single 3D-QSAR CB1 or CB2 model derived from the conformers other than F103 would not help to induce the structural clues to identify the ligand specificity to the CB subtypes.

3D-QSAR Models of Antagonist Binding to the CB1 Receptor. To build a 3D-QSAR model of antagonists binding to the CB1 receptor, a total of 29 arylpyrazoles was included in the cross-validated PLS analysis. Table 5 lists the cross-validated r^2 values in all CoMFA analyses by using templates of five conformers of AM263. The CoMFA study, based on conformer F103, which was the preferred AM263 conformation that was determined from NMR and molecular modeling, gave

Table 5. Cross-Validated Analyses of the CB1 CoMFA Model Based on Four Low-Energy AM263 Conformers as Templates

model	template conformation	compd	r_{cv}^2	optimal component
A	F103	**29**	0.697	5
B	F36	**29**	0.503	4
C	F53	**29**	0.563	5
D	F70	**29**	0.509	4
E	F115	**29**	0.648	4

Table 6. Cross-Validated Analyses of the CB2 CoMFA Models Based on Four Low-Energy AM263 Conformers as Templates

model	template conformation	compd	r_{cv}^2	optimal component
A	F103	**28**	0.641	4
B	F36	**28**	0.614	4
C	F53	**28**	0.531	2
D	F70	**28**	0.588	3
E	F115	**28**	0.564	5

Table 7. Experimental (obsd) and CoMFA-predicted (pred) pK_i Values (nM) of Molecules in the Training Set for CB1 and CB2 Receptors

|	CB1 CoMFA model	CB2 CoMFA model
r^2	0.958	0.977
standard error of estimate	0.200	0.182
F	83.878	147.881
P	<0.0001	<0.0001

	CB1 CoMFA model			CB2 CoMFA model		
compd	pK_i(obsd)	pK_i(pred)	residual	pK_i(obsd)	pK_i(pred)	residual
1 (SR141716A)	7.94	7.65	0.29	5.78	5.99	−0.21
2	7.42	7.12	0.30	6.14	6.14	−0.0048
3	6.91	7.18	−0.27	6.66	6.51	0.15
4	6.69	6.72	−0.02	−	−	−
5	7.77	7.74	0.03	5.89	5.66	0.22
6	7.77	7.76	0.01	5.85	5.94	−0.09
7	8.14	8.20	−0.06	6.14	6.20	−0.06
8	7.12	6.97	0.15	5.90	5.83	0.07
9	6.90	6.84	0.07	5.34	5.39	−0.05
10	6.77	6.71	0.06	4.96	4.93	0.03
11	6.80	6.81	−0.01	4.51	4.41	0.09
12	4.46	4.66	−0.20	4.27	4.18	0.10
13	5.44	5.36	0.08	5.81	5.98	−0.17
14 (AM263)	7.95	7.67	0.28	7.57	7.25	0.32
15	6.69	6.69	−0.0016	6.47	6.62	−0.16
16	6.22	6.09	0.13	5.84	6.05	−0.21
17	7.09	7.39	−0.31	6.28	6.52	−0.25
18	6.59	6.51	0.08	7.04	7.01	0.04
19	6.49	6.34	0.15	7.08	6.92	0.16
20	7.22	7.38	−0.15	6.08	6.02	0.06
21	6.74	6.79	−0.05	6.13	6.24	−0.12
22	7.24	7.51	−0.27	6.60	6.17	0.43
23	7.09	7.53	−0.44	6.02	6.12	−0.1
24	7.88	7.91	−0.03	5.38	5.49	−0.12
25	7.93	7.92	0.01	6.00	6.01	−0.01
26	8.13	7.94	0.19	5.64	5.78	−0.14
27 (SR144528)	6.40	6.40	−0.0048	9.22	9.22	0.0038
28	8.30	8.34	−0.04	7.12	7.04	0.08
29	8.22	8.19	0.04	8.60	8.68	−0.08

rise to the highest cross-validated r^2 values of 0.697, surpassing the generally accepted criterion for statistical validity of $r_{cv}^2 > 0.6$. The non-cross-validated PLS analysis yielded an r^2 of 0.958, and the estimated standard error was 0.200 (Table 7). Therefore, the CoMFA-generated 3D-QSAR model for the affinities at the CB1 receptor has a good cross-validated correlation. Such results indicate that the pharmacophore model would highly fit the training set data, which was realized when the model was employed to calculate the affinities of the ligands in the training set (Table 7). Figure 5A shows the relationship between the calculated and measured K_i values for the non-cross-validated
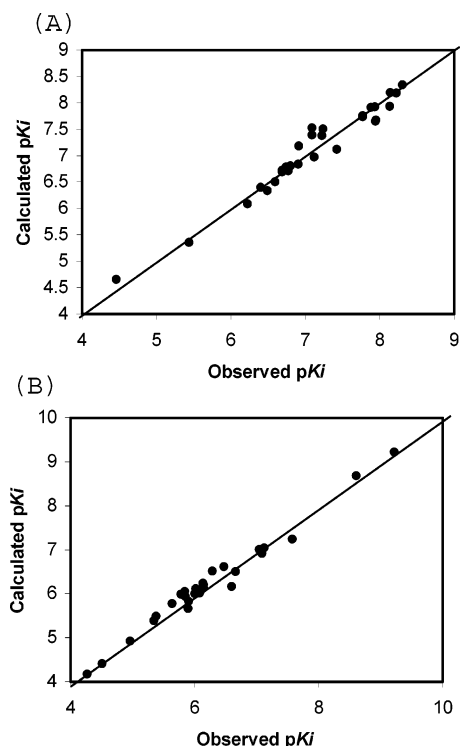
Figure 5. Plots of the corresponding CoMFA-calculated and experimental values of binding affinity (given as pK_i) of arylpyrazole compounds in the training set at the CB1 (A) and CB2 (B) receptor, respectively.

CB1 analysis. The linearity of the plot demonstrated a very good correlation for the CoMFA model developed in the study for the binding affinities of arylpyrazoles at the CB1 receptor site.

3D-QSAR Models of Antagonist Binding to the CB2 Receptor. Twenty-eight ligands were included in the CoMFA analyses to build the 3D-QSAR model for arylpyrazole binding to the CB2 receptor. As with the CB1 receptor, Table 6 lists the cross-validated r_{cv}^2 values and optimal components for all different CoMFA analyses. These analyses also led to the conclusion that CoMFA analysis based on conformer F103 as a template conformation has the highest cross-validated r_{cv}^2 values. The non-cross-validated PLS analysis yielded a r^2 of 0.977 and the standard error of estimate was 0.182 (Table 7). Figure 5B shows the linear relationship between actual pK_i values for compounds in the training set and the fitted values generated by the CoMFA model for the non-cross-validated (r^2) CB2 analysis.

The predictive power of both CB1 and CB2 CoMFA models derived above was evaluated and examined by using a test set of nine molecules that were selected from the literature.[28,32,41] As shown in Table 8, in both models, the predicted values fall close to the actual pK_i values, not deviating by more than 1 logarithmic unit except for two compounds in the test set. Molecules **T6** and **T8** are outliers (residual more than 1.0) in the prediction from the CB1 3D-QSAR model.

CoMFA Contour Maps. Figure 6 shows the steric–electrostatic contour maps of the CoMFA models for the CB1 (A) and CB2 (B) receptors. The individual contributions from the steric and electrostatic fields were 80% and 20% for both CB1 and CB2 CoMFA models, respectively. The CoMFA contour maps depict regions around the molecules where the enhanced CB1 or CB2 cannabinoid receptor binding affinity is associated respectively with respectively increasing (green) and decreasing (yellow) steric bulk regions and with increasing (red) and decreasing (blue) negative charge domains. Figure 6A

Table 8. Experimental (obsd) and CoMFA-predicted (pred) pK_i Values (nM) of Molecules in Test Set for CB1 and CB2 Receptors[a]

compd	CB1 CoMFA model			CB2 CoMFA model		
	pK_i(obsd)	pK_i(pred)	residual	pK_i(obsd)	pK_i(pred)	residual
T1	7.33	7.22	0.11	5.51	5.52	−0.01
T2	6.79	7.10	−0.31	5.90	5.91	−0.01
T3	6.42	6.83	−0.41	4.92	5.29	−0.37
T4	6.84	6.50	0.34	5.22	5.47	−0.25
T5	8.46	7.64	0.82	6.35	6.01	0.34
T6	8.84	7.30	1.54	9.11	8.43	0.68
T7	7.91	7.79	0.12	8.32	8.52	−0.20
T8	8.90	7.31	1.59	9.17	8.77	0.40
T9	7.83	7.79	0.04	7.81	7.93	0.08

[a] The structures of molecules are shown in Table 2.

displays a CoMFA contour map for the arylpyrazole binding to the CB1 receptor. The green areas indicate the regions of favored steric interactions that would enhance binding affinity. The yellow regions are unfavorable areas of steric interactions that would result in reduced binding affinity. On the other hand, the red or blue regions show preferred charged interactions between ligand and receptor. Examination of the model demonstrates that steric effects contributed more to the affinity for the CB1 receptor subtype than the electronic effects. Similarly, the resulting CoMFA contour map displayed in Figure 6B shows the most favored and unfavorable regions of steric and electrostatic interactions for the arylpyrazole ligands with CB2 receptor.

Discussion

The arylpyrazole compound SR141716A is the first selective potent antagonist for the CB1 receptor.[25] It has been reported that memory impairment produced by anandamide can be attenuated by SR141716A.[44] Thomas et al.[24] and Lan et al.[33] separately developed SAR models for arylpyrazoles using a set of SR141716A analogues. The Thomas' SAR model[24] was first reported to be consistent with a pharmacophoric alignment in which the monochloro ring of SR141716A is overlaid with the C-3 alkyl side chain of Δ⁹-THC, the pyrazole nitrogen of SR141716A is overlaid with the C-1 phenolic hydroxyl of Δ⁹-THC, and the carbonyl oxygen of SR141716A is overlaid with the pyran oxygen of Δ⁹-THC. In this superposition, the dichlorophenyl ring of SR141716A represents a region unique to SR141716A, and this region is hypothesized to be the antagonist-conferring moiety of SR141716A. In another SAR study of arylpyrazole SR141716A, Lan et al.[33] identified the structural requirements, including (a) a para-substituted phenyl ring at the 5-position, (b) a carboxamido group at the 3-position, and (c) a 2,4-dichlorophenyl substituent at the 1-position of the pyrazole ring, for bioactive and selective CB1 antagonist activity.

SR144528, also an arylpyrazole derivative, is a selective CB2 antagonist that displays sub-nanomolar affinities for both the rat spleen and cloned human CB2 receptor.[26] It displays a 700-fold higher affinity for both the rat brain and cloned human CB2 receptors than CB1 receptors. SR144528 has recently been shown to act as an inverse agonist at the CB2 receptor.[45] Mutational analysis and molecular modeling of SR144528 suggest that it interacts with residues in transmembrane domains 3, 4, and 5 of the cannabinoid CB2 receptor through a combination of H-bonding, as well as aromatic and hydrophobic interactions.[46] However, the SAR analysis of arylpyrazoles for CB2 selectivity is seldom reported.

The CoMFA analyses were performed to construct 3D-QSAR models of the binding affinities of arylpyrazoles for CB1 and CB2 receptors, respectively, on the basis of AM263's conformations as templates. The experimental design was based on the fact that CoMFA can be extended to a comparative evaluation of different binding affinities of compounds in the same molecular set for two closely related receptors to build differential 3D-QSAR models.[47] At first, the conformational analysis of AM263 was performed by correlating the experimental NMR results with computational data. The chloroform was chosen since it is a nonpolar organic solvent and has been accepted as a NMR solvent media that mimics a hydrophobic membrane environment.[48,49] Our studies involved the analysis of conformational properties of individual molecular components, subsequently combining them to provide a complete picture of the molecule under study. Finally, the preferred solution conformation, as defined by the alignment of the pharmacophoric groups, was determined by maximal agreement between the experimental and computational results.

The NMR solution conformation of AM263 indicates that the amide group in arylpyrazoles exists in the trans-conformation with the torsion angle (N2−C3−C1″−O) of about 180°. The result is congruent with the ab initio calculation results that demonstrated that the energy of the trans-conformation of amide in arylpyrazoles is approximately 10 kcal/mol more lower than that of the cis-conformation.[21] Such a conformation was also consistent with other NMR studies of the arypyrazole compounds.[50,51] A docking study,[52] based on the results indicating that the K3.28(192) site is critical for the inverse agonist activity of SR141716A,[53] also postulated that the carboxamide oxygen of SR141617A with a *trans*-amide conformation forms a hydrogen bond with K3.28(192) in the CB1 receptor. Also, the authors[52] hypothesized that aromatic stacking interactions might be important for the binding of arylpyrazole compounds to CB1 and that both the monochlorophenyl and dichlorophenyl rings of SR141617A were involved in aromatic stacking interactions with aromatic residues including W5.43(279), F3.36(200), and Y5.39(275).

CoMFA is carried out in this study to develop the key pharmacophoric features solely on the basis of ligand structural requirements without consideration for receptor structure. On the basis of five distinct conformations of AM263, five CoMFA models were derived from the CB1 and CB2 K_i values of 29 arylpyrazole compounds. Using the AM263 conformations as templates, the compounds in our training set were superimposed and aligned to meet the SAR requirements with regard to antagonist selectivity for CB1 or CB2 receptors. These pharmacophoric requirements include (a) a para-substituted phenyl ring at C5, (b) a carboxamido group at C3, and (c) a 2,4-dichlorophenyl substituent at the N1 of the pyrazole ring. Our CoMFA analyses based on the preferred solution conformation of AM263 produced the highest cross-validation r^2 values for CB1 and CB2 receptors.

As shown in Figure 6, the field contributions indicate that the variation in binding affinity among the arylpyrazoles is dominated by steric interactions at the receptor site. The result is consistent with the recognized importance of the hydrophobic components of the classical cannabinoids and of the arylpyrazoles for cannabimimetic activity. The contour maps of the CoMFA model demonstrate that there are different structural requirements for arylpyrazole binding to the CB1 and CB2 receptors. For example, the red and green contours in the region around the 5-phenyl para substituent on the pyrazole ring in the CB1 CoMFA model indicate that the presence of a negatively charged bulky group such as halogen is expected to enhance CB1 receptor binding affinity in this region. Con-
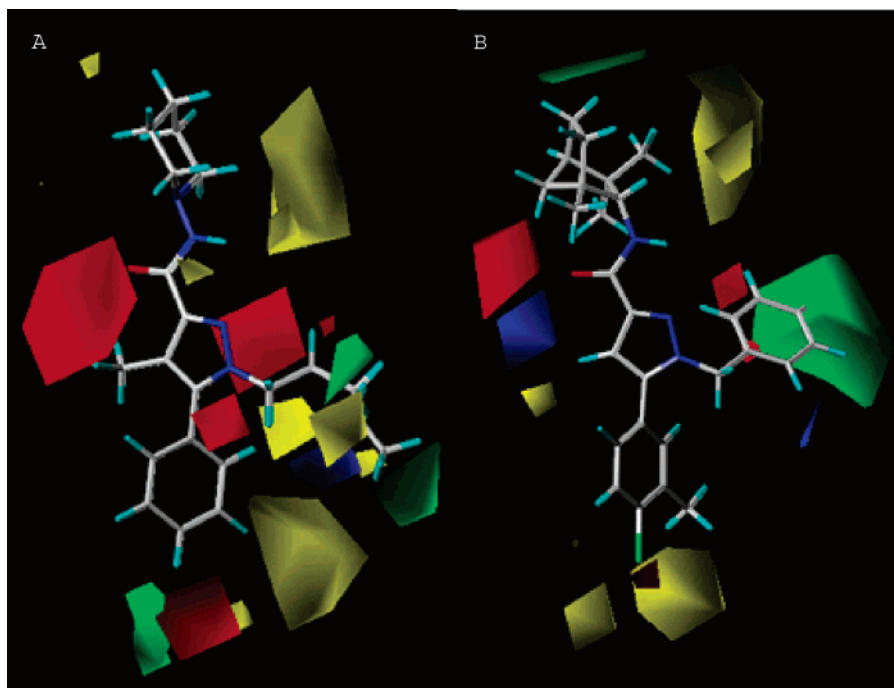
Figure 6. CoMFA contour maps for CB1 (A) and CB2 (B) receptor, respectively. Sterically favored areas (contribution level of 80%) are in green. Sterically unfavored areas (contribution level of 20%) are in yellow. Positive potential favored areas (contribution level of 80%) are in blue. Positive potential unfavored areas (contribution level of 20%) are in red.

versely, in the same region of the CoMFA model for the CB2 receptor, the yellow contour indicates that the presence of bulky groups will weaken the binding affinity of arypyrazoles for the CB2 receptor. For this reason, compound **29** has a stronger binding affinity than compound **28** for the CB2 receptor. The results also imply that the 5-phenyl para substituents of the arylpyrazoles will interact with the CB1 receptor via steric and electrostatic interactions, while at the CB2 receptor only steric interactions are involved. In the region around the end of the *N*-amido substituent, the opposite steric field contours for the CB1 and CB2 were observed in the CoMFA models, suggesting that the steric interactions within these pharmacophores would affect differently the arylpyrazoles' binding affinities for the CB1 and CB2 receptors. The contour maps in the 3D-QSAR model for the CB2 receptor exhibit a green region, which suggests that bulky groups are favored for high CB2 affinity, whereas in the CB1 model map the role of steric interactions is ambiguous. Steric bulk at the distal region of N-amido substituents in arylpyrazoles affords high binding affinity for CB2 but not for CB1. Another interesting pharmacophoric region is related to the 4-substituents. The CB1 CoMFA model has red contours for the 4-methyl region whereas the CB2 model shows blue and yellow contours, indicating that the presence of the 4-methyl group increases the binding affinity for the CB1 receptor but decreases the binding affinity for the CB2 receptor. In the regions proximal to the carbonyl oxygen, both CB1 and CB2 CoMFA models show red contours, indicating that this negatively charged group favors the binding of the arylpyrazoles to both the CB1 and CB2 receptors. In addition, both CB1 and CB2 pharmacophore maps show large yellow contours between the N-substitution of pyrazole ring and N-substitution of amide (or two putative pockets for the receptors). These may represent receptor-essential volumes between the two virtual pockets of cannabinoid receptors.

The generated CoMFA models indicate that the arylpyrazole compounds have different pharmacophoric requirements for the CB1 and CB2 receptors. While bulky electronegative substit-

uents at the C5 position enhance the CB1 selectivity of the ligand, such substitutions in the position are especially unfavorable for CB2 binding. This is clearly demonstrated by compounds **24**−**26** in our training set, which exhibit higher CB1 selectivity, whereas compound **29**, which lacks 5-phenyl ring substitution, has better CB2 selectivity. Substitution, at the N1 position of arylpyrazoles seems to require the presence of bulky groups. However, the CoMFA contour maps reveal that larger N1-substituents favor the CB2 receptor. We can postulate the presence of a larger hydrophobic cavity in CB2 binding site capable of accommodating larger hydrophobic groups. Another interesting feature that modulates CB1/CB2 selectivity is the presence of the C4-methyl group. As shown in Table 1, compounds with the C4-methyl groups tend to favor CB1 affinity, whereas compounds lacking the C4-methyl tend to be more CB2-selective. However, the CoMFA studies did not provide any insights as to why the presence of the relatively small methyl group can influence arylpyrazole selectivity for CB1.

In summary, the present work describes the first successful attempt to conduct a NMR-based 3D-QSAR/CoMFA study of the CB1 and CB2 pyrazole antagonist pharmacophore models. Using the NMR-determined preferred ligand conformations as templates, more general CB1 and CB2 PLS pharmacophore models were developed, which fitted our experimental binding data with a high correlation coefficient. Also, the congruency of the CoMFA predicted the bioactive conformation with the arylprazole's solution conformation, and this supports these models as representing the bioactive conformation at the CB1 and CB2 sites. Our CoMFA analyses based on binding affinity data of arylpyrazole ligands for the CB1 and CB2 receptors allowed us to deduce the possible CB1 and CB2 binding information for arylpyrazoles that describe the optimal substitution at the N1, C3, C4, and C5 positions. In addition, since 3D structures of the cannabinoid receptors are not available, the deduced 3D-QSAR models would further be tested through predictions for an accurate reflection of the ligand orientations

at the receptors. Generally, the created CoMFA models may serve as guides for understanding the binding characteristics of arylpyrazoles at the CB1 and CB2 receptor binding sites and also serve as aides in the design of later-generation analogues.

References

(1) Matsuda, L. A.; Bonner, T. I.; Lolait, S. J. Localization of cannabinoid receptor mRNA in rat brain. *J. Comput. Neurol.* **1993**, *327*, 535−550.

(2) Matsuda, L. A.; Lolait, S. J.; Brownstein, M. J.; Young, A. C.; Bonner, T. I. Structures of a cannabinoid receptor and functional expression of the cloned cDNA. *Nature (London)* **1990**, *346*, 561−564.

(3) Herkenham, M.; Lynn, A. B.; Johnson, M. R.; Melvin, L. S.; de Costa, B. R.; Rice, K. C. Characterization and localization of cannabinoid receptors in rat brain: A quantitative in vitro autoradiographic study. *J. Neurosci.* **1991**, *11*, 563−583.

(4) Munro, S.; Thomas, K. L.; Abu-Shaar, M. Molecular characterization of a peripheral receptor for cannabinoids. *Nature (London)* **1993**, *365*, (64411), 61−65.

(5) Galiegue, S.; Mary, S.; Marchand, J.; Dussossoy, D.; Carriere, D.; Carayon, P.; Bouaboula, M.; Shire, D.; Le Fur, G.; Casellas, P. Expression of central and peripheral cannabinoid receptors in human immune tissues and leukocyte subpopulations. *Eur. J. Biochem.* **1995**, *232*, 54−61.

(6) Razdan, R. K.; Howes, J. F. Drugs related to tetrahydrocannabinol. *Med. Res. Rev.* **1983**, *3*, 119−146.

(7) Segal, M., Cannabinoids and Analgesia. In *Cannabinoids as Herapeutic Agents*; Mechoulam, R., Ed.; CRC Press: Boca Raton, FL, 1986; pp 105−120.

(8) Pertwee, R. G. Pharmacology of cannabinoid CB1 and CB2 receptors. *Pharmacol. Ther.* **1997**, *74*, 129−80.

(9) Pertwee, R. G. The central neuropharmacology of psychotropic cannabinoids. *Pharmacol. Ther.* **1988**, *36*, 189−261.

(10) Hollister, L. E. Health aspects of cannabis. *Pharmacol. Rev.* **1986**, *38*, 1−20.

(11) Dewey, W. L. Cannabinoid pharmacology. *Pharmacol. Rev.* **1986**, *38*, 151−178.

(12) Huffman, J. W. The search for selective ligands for the CB2 receptor. *Curr. Pharm. Des.* **2000**, *6*, 1323−1337.

(13) Pertwee, R. G. Pharmacology of cannabinoid receptor ligands. *Curr. Med. Chem.* **1999**, *6*, 635−664.

(14) Reggio, P. H. Pharmacophores for ligand recognition and activation/inactivation of the cannabinoid receptors. *Curr. Pharm. Des.* **2003**, *9*, 1607−1633.

(15) Cramer, R. D. I.; DePriest, S.; Patterson, D.; Hecht, P. The developing practice of comparative molecular field analysis. In *3D QSAR in Drug Design*; Kubinyi, H., Ed.; ESCOM: Leiden, 1993; pp 443−485.

(16) Thomas, B. F.; Compton, D. R.; Martin, B. R.; Semus, S. F. Modeling the cannabinoid receptor: A three-dimensional quantitative structure−activity analysis. *Mol. Pharmacol.* **1991**, *40*, 656−65.

(17) Schmetzer, S.; Greenidge, P.; Kovar, K.-A.; Schulze-Alexandru, M.; Folkers, G. Structure−activity relationships of cannabinoids: A joint CoMFA and pseudoreceptor modeling study. *J. Comput.-Aided Mol. Des.* **1997**, *11*, 278−292.

(18) Shim, J.-Y.; Collantes, E. R.; Welsh, W. J.; Subramaniam, B.; Howlett, A. C.; Eissenstat, M. A.; Ward, S. J. Three-dimensional quantitative structure−activity relationship study of the cannabimimetic (aminoalkyl)indoles using comparative molecular field analysis. *J. Med. Chem.* **1998**, *41*, 4521−4532.

(19) Thomas, B. F.; Adams, I. B.; Mascarella, S. W.; Martin, B. R.; Razdan, R. K. Structure−activity analysis of anandamide analogues: Relationship to a cannabinoid pharmacophore. *J. Med. Chem.* **1996**, *39*, 471−479.

(20) Tong, W.; Collantes, E. R.; Welsh, W. J.; Berglund, B. A.; Howlett, A. C. Derivation of a pharmacophore model for anandamide using constrained conformational searching and comparative molecular field analysis. *J. Med. Chem.* **1998**, *41*, 4207−4215.

(21) Shim, J.-Y.; Welsh, W. J.; Cartier, E.; Edwards, J. L.; Howlett, A. C. Molecular interaction of the antagonist *N*-(Piperidin-1-yl)-5-(4-chlorophenyl)-1-(2,4-dichlorophenyl)-4-methyl-1H-pyrazole-3-carboxamide with the CB1 cannabinoid recptor. *J. Med. Chem.* **2002**, *45*, 1447−1459.

(22) Fichera, M.; Cruciani, G.; Bianchi, A.; Musumarra, G. A 3D-QSAR study on the structural requirements for binding to CB1 and CB2 cannabinoid receptors. *J. Med. Chem.* **2000**, *43*, 2300−2309.

(23) Song, Z. H.; Slowey, C.-A.; Hurst, D. P.; Reggio, P. H. The difference between the CB1 and CB2 cannabinoid receptors at position 5.46 is crucial for the selectivity of WIN55212-2 for CB2. *Mol. Pharmacol.* **1999**, *56*, 834−840.

(24) Thomas, B. F.; Gilliam, A. F.; Burch, D. F.; Roche, M. J.; Seltzman, H. H. Comparative receptor binding analyses of cannabinoid agonists and antagonists. *J. Pharmacol. Exp. Ther.* **1998**, *285*, 285−292.

(25) Rinaldi-Carmona, M.; Barth, F.; Heaulme, M.; Shire, D.; Calandra, B.; Congy, C.; Martinez, S.; Maruani, J.; Neliat, G. SR141716A, a potent and selective antagonist of the brain cannabinoid receptor. *FEBS Lett.* **1994**, *350*, 240−244.

(26) Rinaldi-Carmona, M.; Barth, F.; Millan, J.; Derocq, J.-M.; Casellas, P.; Congy, C.; Oustric, D.; Sarran, M.; Bouaboula, M.; Calandra, B.; Portier, M.; Shire, D.; Brelière, J.-C.; L., F. G. SR 144528, the first potent and selective antagonist of the CB2 cannabinoid receptor. *J. Pharmacol. Exp. Ther.* **1998**, *284*, 644−650.

(27) Dow, R. L.; Hammond, M. Preparation of pyrazoles and imidazoles as cannabinoid CB1 receptor antagonists. PCT Int. Appl. WO 2004052864, 2004.

(28) Makriyannis, A.; Liu, Q. Preparation of pyrazole derivatives as cannabinoid receptor antagonists. PCT Int. Appl. WO 2001029007, 2001.

(29) Martin, B. R.; Razdan, R. K.; Mahadevan, A. Preparation of pyrazoles as cannabnoid agonists and antagonists. PCT US 6509367, 2003.

(30) Mussinu, J. M.; Ruiu, S.; Mule, A. C.; Pau, A.; Carai, M. A.; Loriga, G.; Murineddu, G.; Pinna, G. A. Tricyclic pyrazoles. Part 1: Synthesis and biological evaluation of novel 1,4-dihydroindeno[1,2-*c*]-based ligands for CB1 and CB2 cannabinoid receptors. *Bioorg. Med. Chem.* **2003**, *11*, 251−263.

(31) Katoch-Rouse, R.; Pavlova, O. A.; Caulder, T.; Hoffman, A. F.; Mukhin, A. G.; Horti, A. G. Synthesis, sturcture−activity relationship, and evaluation of SR141716 analogues: Development of central cannabinoid receptor ligands with lower lipophilicity. *J. Med. Chem.* **2003**, *46*, 642−645.

(32) Francisco, M. E. Y.; Elena, Y.; Seltzman, H. H.; Herbert, H.; Gilliam, A. F.; Mitchell, R. A.; Rider, S. L.; Pertwee, R. G.; Stevenson, L. A.; Thomas, B. F. Synthesis and structure−activity relationships of amide and hydrazide analogues of the cannabinoid CB1 receptor antagonists *N*-(piperidinyl)-5-(4-chlorophenyl)-1-(2,4-dichlorophenyl)-4-methyl-1*H*-pyrazole-3-carboxamide (SR141716). *J. Med. Chem.* **2002**, *45*, 2708−2719.

(33) Lan, R.; Liu, Q.; Fan, P.; Lin, S.; Fernando, S. R.; McCallion, D.; Pertwee, R.; Makriyannis, A. Structure−activity relationships of pyrazole derivatives as cannabinoid receptor antagonists. *J. Med. Chem.* **1999**, *42*, (4), 769−776.

(34) Marion, D.; Wüthrich, K. Application of phase sensitive two-dimensional correlated spectroscopy (COSY) for measurements of proton−proton spin−spin coupling constants in proteins. *Biochem. Biophys. Res. Commun.* **1983**, *113*, (3), 967−974.

(35) Bodenhausen, G.; Kogler, H.; Ernst, R. R. Selection of coherence-transfer pathways in NMR pulse experiments. *J. Magn. Reson.* **1984**, *58*, (3), 370−388.

(36) Bax, A.; Subramanian, S. Sensitivity-enhanced two-dimensional heteronuclear shift correlation NMR spectroscopy. *J. Magn. Reson.* **1986**, *67*, (3), 565−569.

(37) Ruiz-Cabello, J.; Vuister, G. W.; Moonen, C. T. W.; Van Gelderen, P.; Cohen, J. S.; Van Zijl, P. C. M. Gradient-enhanced heteronuclear correlation spectroscopy. Theory and experimental aspects. *J. Magn. Reson.* **1992**, *100*, (2), 282−302.

(38) *Sybyl molecular modeling software packages*, ver. 6.8; TRIPOS, Associates, Inc.: St Louis, MO 63144, 2001.

(39) Muir, K. W.; Morris, D. G. *N*,*N*-Dimethyl-*N*′-(*o*-fluorobenzoyl)-hydrazide. *Acta Crystallogr. E* **2003**, *E59*, o490−o492.

(40) Prasad, S. M.; Ammon, H. L.; Mahto, R. D. Structure of *N*′,*N*′-dibenzylbenzohydrazide. *Acta Crystallogr. C* **1990**, *C46*, 2267−2268.

(41) Rinaldi-Carmona, M.; Barth, F.; Congy, C.; Martinez, S.; Oustric, D.; Pério, A.; Poncelet, M.; Maruani, J.; Arnone, M.; Finance, O.; Soubrié, P.; Le Fur, G. SR147778 [5-(4-bromophenyl)-1-(2,4-dichlorophenyl)-4-ethyl-*N*-(1-piperidinyl)-1*H*-pyrazole-3-carboxamide], a new potent and selective antagonist of the CB1 cannabinoid receptor: Biochemical and pharmacological characterization. *J. Pharmacol. Exp. Ther.* **2004**, *310*, 905−914.

(42) Xie, X.-Q.; Melvin, L. S.; Makriyannis, A. The conformational properties of the highly selective cannabinoid receptor ligand CP-55,940. *J. Biol. Chem.* **1996**, *271* (181), 10640−10647.

(43) Dunn, W. J.; Wold, S.; Edlund, V.; Helberg, S. Multivariate structure−activity relationships between data from a battery of biological tests and an ensemble of structure descriptors: The PLS method. *Quantum Struct.−Act. Relat.* **1984**, *3*, 131−137.

(44) Mallet, P. E.; Beninger, R. J. The cannabinoid CB1 receptor antagonist SR141716A attenuates the memory impairment produced by delta9-tetrahydrocannabinol or anandamide. *Psychopharmacology (Berlin)* **1998**, *140*, 11−19.

(45) Bouaboula, M.; Desnoyer, N.; Carayon, P.; Combes, T.; Casellas, P. Gi protein modulation induced by a selective inverse agonist for the peripheral cannabinoid receptor CB2: Implication for intracellular signalization cross-regulation. *Mol. Pharmacol.* **1999**, *55*, 473−480.

(46) Gouldson, P.; Calandra, B.; Legoux, P.; Kerneis, A.; Rinaldi-Carmona, M.; Barth, F.; Le Fur, G.; Ferrara, P.; Shire, D. Mutational analysis and molecular modeling of the antagonist SR 144528 binding site on the human cannabinoid CB2 receptor. *Eur. J. Pharmacol.* **2000**, *401*, 17−25.

(47) Wilcox, R. E.; Tseng, T.; Brusniak, M. Y.; Ginsburg, B.; Pearlman, R. S.; Teeter, M.; DuRand, C.; Starr, S.; Neve, K. A. CoMFA-based prediction of agonist affinities at recombinant D1 vs D2 dopamine receptors. *J. Med. Chem.* **1998**, *41*, 4385−99.

(48) Arseniev, A. S.; Barsukov, I. L.; Bystrov, V. F.; Lomize, A. L.; Ovchinnikov, Y. A. 1H NMR study of gramcidin A transmembrane ion channel head to head right handed single stranded helices. *FEBS* **1985**, *186*, 168−174.

(49) Pervushin, K. V.; Orekhov, V. Y.; Popov, A. I.; Musina, L. Y.; Arseniev, A. S., Three-dimensional structure of (1−71)bacterioopsin solubilized in methanol/chloroform and SDS micelles determined by nitrogen-15-proton heteronuclear NMR spectroscopy. *Eur. J. Biochem.* **1994**, *219*, 571−83.

(50) Francisco, M. E. Y.; Burgess, J. P.; George, C.; Bailey, G.; Gilliam, A. F.; Seltzman, H. H.; Thomas, B. F. Structure elucidation of a novel ring-constrainted biaryl pyrazole CB1 cannabinoid receptor antagonist. *Magn. Reson. Chem.* **2003**, *41*, 265−268.

(51) Krishnamurthy, M.; Li, W.; Moore, B. M. Synthesis, biological evaluation, and structural studies on N1 and C5 substituted cycloalkyl analogues of the pyrazole class of CB1 and CB2 ligands. *Bioorg. Med. Chem.* **2004**, *12*, 393−404.

(52) Hurst, D. P.; Lynch, D. L.; Barnett-Norris, J.; Hyatt, S. M.; Seltzman, H.; H.; Zhong, M.; Song, Z.-H.; Nie, J.; Lewis, D.; Reggio, P. H. *N*-(Piperidin-1-yl)-5-(4-chlorophenyl)-1-(2,4-dichlorophenyl)-4-methyl-1*H*-pyrazole-3-carboxamide (SR141716A) interaction with LYS 3.28(192) is crucial for its inverse agonism at the cannabinoid CB1 receptor. *Mol. Pharmacol.* **2002**, *62*, 1274−1287.

(53) Pan, X.; Ikeda, S. R.; Lewis, D. L. SR141716A acts as an inverse agonist to increase neuronal voltage-dependent Ca^{2+} currents by reversal of tonic CB1 receptor activity. *Mol. Pharmacol.* **1998**, *54*, 1064−1072.